High-Efficiency Space and Terrestrial Multijunction Solar Cells Through Bandgap Control in Cell Structures

Richard R. King, Chris M. Fetzer, Peter C. Colter, Ken M. Edmondson, James H. Ermer, Hector L. Cotal, Hojun Yoon, Alex P. Stavrides, Geoff Kinsey, Dimitri D. Krut, N. H. Karam

Spectrolab, Inc., 12500 Gladstone Ave., Sylmar, CA 91342

ABSTRACT

Using the energy bandgap of semiconductors as a design parameter is critically important for achieving the highest efficiency multijunction solar cells. The bandgaps of lattice-matched semiconductors that are most convenient to use are rarely those which would result in the highest theoretical efficiency. For both the space and terrestrial solar spectra, the efficiency of 3-junction GaInP/GaAs/Ge solar cells can be increased by a lower bandgap middle cell, as for GaInAs middle cells, as well as by using higher bandgap top cell materials. Wide-bandgap and indirect-gap materials used in parasitically absorbing layers such as tunnel junctions help to increase transmission of light to the active cell layers beneath. Control of bandgap in such cell structures has been instrumental in achieving solar cell efficiencies of 29.7% under the AM0 space spectrum (0.1353 W/cm^2, 28^{o}C) and 34% under the concentrated terrestrial spectrum (AM1.5G, 150-400 suns, 25^{o}C), the highest yet achieved for solar cells built on a single substrate.

INTRODUCTION

GaInP/GaAs/Ge triple-junction solar cells benefit from their use of a combination of semiconductors that can be grown with a high degree of crystal quality, and also have a wide range of bandgaps allowing efficient conversion of both the space and terrestrial solar spectra[1,2]. As a result, this type of solar cell is the most efficient cell yet produced on a single growth substrate. However, parts of conventional 3-junction cells are still unoptimized, and the efficiency can be further increased by addressing these areas.

For example, the bandgaps of the Ge substrate, GaAs, and GaInP lattice-matched to GaAs are not ideal for our sun's spectrum. Fig. 1 shows the measured external quantum efficiency (EQE) for each of the three subcells of a high-efficiency 3-junction cell, superimposed on the AM0 space and AM1.5G terrestrial spectra. The spectra are plotted as current density per unit photon energy that would be photogenerated if every photon created an electron hole pair, *i.e.*, $q\widetilde{F}(E)$, where q is the electronic charge, E is the photon energy, and $\widetilde{F}(E)$ is the photon flux per unit photon energy. To achieve equal photogenerated current densities in the top and middle subcells, the integral over, say, the AM1.5G spectrum,

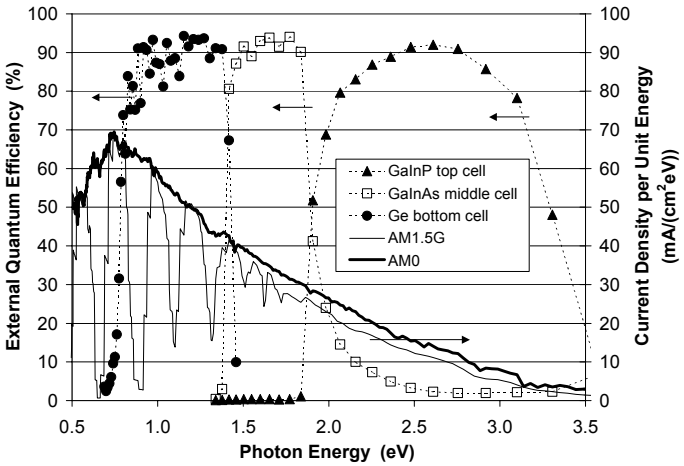

Fig. 1. External quantum efficiency of a high-efficiency GaInP/1%-In GaInAs/Ge 3-junction cell with a wide bandgap top cell and tunnel junction, plotted versus photon energy. The current density per unit photon energy is plotted for comparison, for the AM0 and the AM1.5G spectra.

weighted by the subcell external quantum efficiency $Q(E)$, must be the same for each subcell:

$$J_{\text{ph,top}} = J_{\text{ph,mid}} = \int_0^\infty q\widetilde{F}_{\text{AM1.5G}}(E)\,Q_{\text{top}}(E)\,dE = \int_0^\infty q\widetilde{F}_{\text{AM1.5G}}(E)\,Q_{\text{mid}}(E)\,dE \quad (1)$$

where J_{ph} is the photogenerated current density. This is a reasonable approximation for current matching, though it is actually the current density at maximum power J_{mp} that should be equated among current-matched subcells. For a GaInP top cell lattice-matched to GaAs, this constraint requires the top cell to be made more transparent to the incident light, either by increasing its bandgap to the greatest extent possible by group-III sublattice disordering, or by thinning the top cell substantially, in order to allow enough light through to the GaAs middle subcell for current matching. Increasing the bandgap of the top subcell is a preferred way to increase the transmission of light to the middle cell, since it increases the voltage of the top cell, rather than simply wasting photons that could generate electron-hole pairs in a thinned GaInP subcell with no compensating voltage gain.

The Ge subcell situated beneath the GaAs subcell has excess photogenerated current density, roughly two times that required for current match to the top two subcells. This opens up the possibility of higher efficiency conversion by lowering the bandgap and collecting more current in the middle cell, as in the metamorphic GaInP/GaInAs/Ge cell approach[3,4] shown in Fig. 2, or by inserting an additional subcell with a bandgap intermediate between that of GaAs and Ge, as in a GaInP/GaAs/~1.0-eV GaInNAs/Ge 4-junction cell[5-8].

Structures in the multijunction (MJ) cell such as the tunnel junction, window, and back-surface field (BSF) layers can have poor minority-carrier collection properties, so that electron-hole pairs generated there do not fully contribute to the multijunction cell current. The high doping concentration in the tunnel junction layers and proximity to the minority-carrier sink that occurs at the p^{++}/n^{++} tunnel junction interface seriously limits the ability to improve the carrier collection in tunnel junction layers. Window and BSF layers are also preferably heavily doped, and frequently use Al with its attendant high oxygen incorporation, impairing efforts to improve minority-carrier collection in these layers as well. In addition to reducing the layer thickness, increasing the bandgap is an effective way to minimize photogeneration in these layers, and avoid the collection problems by transmitting more photons to the subcell beneath.

The above areas of improvement for GaInP/GaAs/Ge cell design all depend on influencing the bandgap of various layers in the MJ cell, while maintaining a high degree of lattice matching and crystallinity in the cell structures. Control of the bandgap and crystallinity of cell layers has pushed the efficiency of 3-junction GaInP/GaAs/Ge cells to new heights, as described in the sections below.

RESULTS AND DISCUSSION

Top and Middle Cell Bandgaps

The optimum top cell bandgap of a 3-junction cell in which the bottom two cells are GaAs and Ge occurs at ~1.9 eV for the terrestrial solar spectrum and at ~2.0 eV for the AM0 space spectrum[9]. This is considerably higher than the 1.80-eV bandgap of $Ga_{0.51}In_{0.49}P$ lattice-matched to GaAs and ordered on the group-III sublattice. Various methods can be used to disorder or partially disorder the group-III sublattice of the GaInP top cell base and emitter, thereby increasing the GaInP bandgap up to 100 meV. Disordering of the GaInP sublattice is also effective at bringing up the top cell bandgap for higher indium compositions, for instance, in $Ga_{0.44}In_{0.56}P$ lattice-matched to an 8%-In GaInAs middle cell in metamorphic cell designs. In such 3-junction GaInP/GaInAs/Ge cells, the theoretical efficiency is enhanced by the shift of the top and middle cell bandgap combination possible at the larger lattice constant of $Ga_{0.92}In_{0.08}As$, and further increased by the larger top cell bandgap achieved by disordering the $Ga_{0.44}In_{0.56}P$ top cell.

The amount of ordering on the group-III sublattice can be observed directly by measuring the ½(115) x-ray

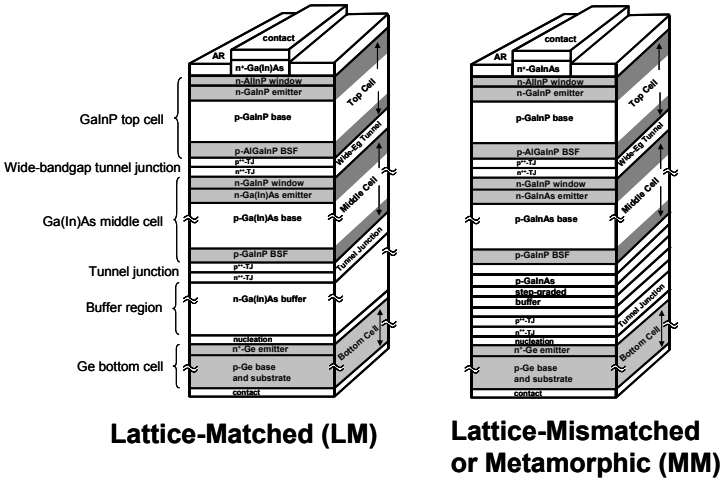

Fig. 2. Cross-sectional diagrams of lattice-matched and metamorphic 3-junction GaInP/GaInAs/Ge solar cells.

diffraction (XRD) peak resulting from the doubling of the unit cell size when Ga and In are ordered in GaInP. The intensity of the ½(115) peak is shown in Fig. 3 for both ordered and disordered samples of GaInP lattice-matched to a Ge substrate, and GaInP lattice-matched to 8%-In GaInAs. The near-zero intensity in the disordered case indicates almost complete disordering of the Ga and In for these samples. The effect of disorder on the bandgap of these samples can be observed in the wavelength-resolved photoluminescence (PL) spectra from these samples in Fig. 4. When the lattice constant and In mole fraction are well characterized using conventional XRD, the energy of the PL peak provides an indirect, but convenient, method of determining the amount of disorder in GaInP.

Minority-carrier lifetime is one of the most important semiconductor parameters for efficient solar cell operation, influencing open-circuit voltage V_{oc}, short-circuit current density, J_{sc}, and fill factor FF. The samples in Figs. 3 and

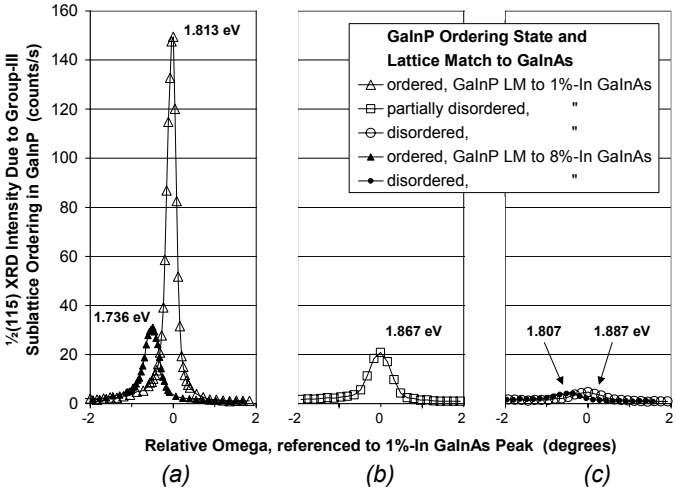

Fig. 3. Measurement of the ½(115) XRD peak due to group-III sublattice ordering, in AlGaInP/GaInP/AlGaInP double heterostructures, for which the GaInP base is lattice-matched to $Ga_{0.99}In_{0.01}As$ or $Ga_{0.92}In_{0.08}As$. The bandgap of the GaInP base is noted next to the peaks.

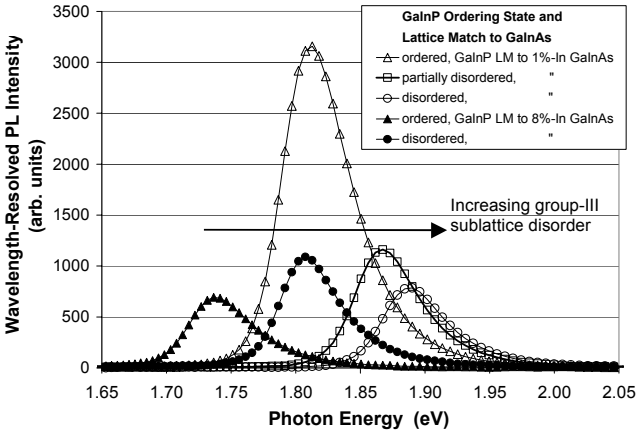

Fig. 4. Photoluminescence of AlGaInP/GaInP/AlGaInP double heterostructures, showing the dependence of GaInP bandgap on sublattice disorder, as well as indium composition in the GaInP base.

4 are AlGaInP/GaInP/AlGaInP double heterostructures (DHs) grown on Ge, for measurement of minority-carrier lifetime by time-resolved photoluminescence (TRPL). The Al composition in the AlGaInP barriers is ~50% of the Ga mole fraction in the GaInP base, *e.g.*, $Al_{0.25}Ga_{0.25}In_{0.50}P$ barriers on $Ga_{0.50}In_{0.50}P$ bases lattice-matched to Ge and to 1%-In GaInAs. GaInP/GaInAs/GaInP DHs were also grown with various In compositions in the GaInAs base, to characterize the lifetime in GaInAs. These structures simulate the base and base/BSF interface in the top and middle subcells of 3-junction cells, and closely mirror the structure of such cells shown in Fig. 2. The TRPL measurements were made at the National Renewable Energy Laboratory (NREL).

Fig. 5 shows TRPL decay curves for a not-intentionally-doped (nid) $Ga_{0.50}In_{0.50}P$-base DH with a 47 ns minority-carrier lifetime, and for a $Ga_{0.99}In_{0.01}As$-base DH with a very long lifetime of 2450 ns. This is far longer than typical lifetimes in GaAs grown on Ge. The GaInP and GaInAs compositions above are chosen to be closely lattice-matched to Ge, and therefore have a lower dislocation density than GaAs on Ge. The lifetimes of 0%-In (GaAs), 1%-In GaInAs, and 8%-In GaInAs, and of GaInP lattice-matched to these compositions, are plotted in Fig. 6. As noted above, the lifetime of 1%-In GaInAs on Ge is far longer than that of GaAs, while 8%-In GaInAs has a lifetime that is only slightly shorter than that of GaAs on Ge. The lifetime of GaInP benefits from close lattice matching to Ge, but to a lower extent than the GaInAs-base DHs.

The lifetime measured by TRPL on DHs, as shown in Fig. 5, is referred to as the effective lifetime τ_{eff} , since it depends on the bulk lifetime τ_{bulk} in the base material, and the interface recombination velocity s at the base/barrier interfaces. The values of τ_{bulk} and s can be extracted by measuring τ_{eff} for DHs with more than one base thickness w. The dependence of τ_{eff} on w is given by:

$$\frac{1}{\tau_{\text{eff}}} = \frac{1}{\tau_{\text{bulk}}} + \frac{2}{w}s = \frac{1}{\tau_{\text{bulk,rad}}} + \frac{1}{\tau_{\text{bulk,SRH}}} + \frac{2}{w}s \qquad (2)$$

where $\tau_{bulk,rad}$ and $\tau_{bulk,SRH}$ are the characteristic bulk lifetimes of radiative and Shockley-Read-Hall (SRH)

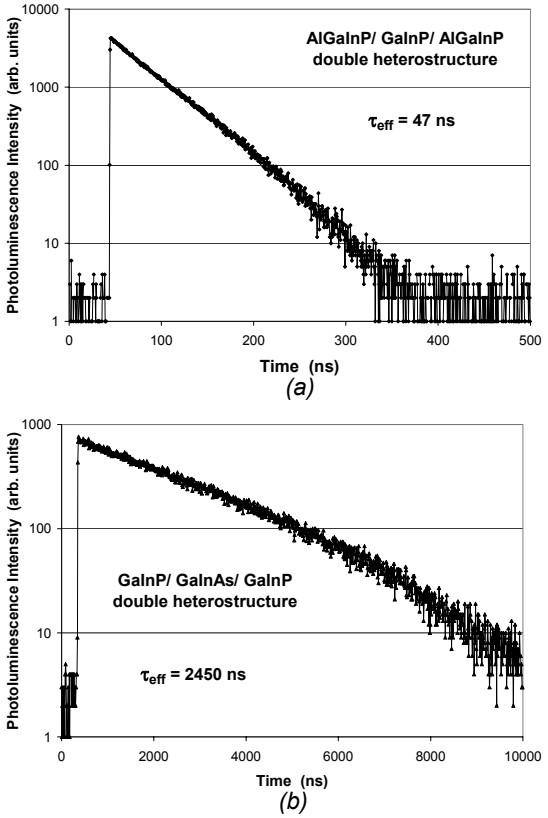

Fig. 5. Time-resolved photoluminescence of double heterostructures: (a) AlGaInP/GaInP/AlGaInP with 47 ns minority-carrier lifetime in the GaInP base lattice-matched to Ge; and (b) GaInP/$Ga_{0.99}In_{0.01}As$/GaInP with bulk lifetime exceeding 2450 ns in the 1%-In GaInAs base.

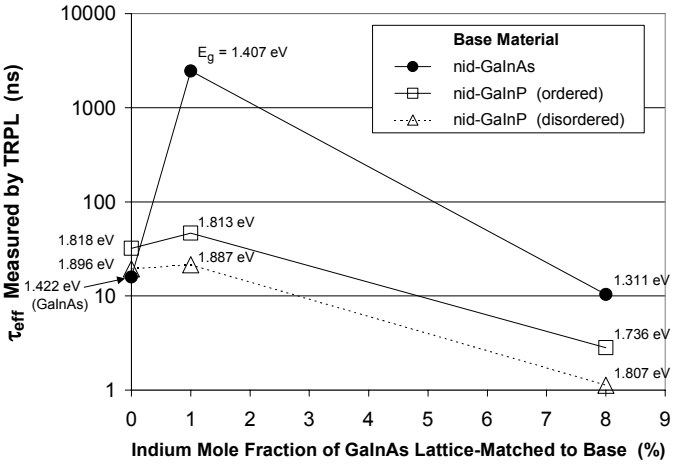

Fig. 6. Dependence of lifetime measured by TRPL in AlGaInP/GaInP/AlGaInP and GaInP/GaInAs/GaInP double heterostructures on indium composition in the base.

recombination, respectively, in the base. The interface recombination characterized by s is considered to take place by the SRH mechanism. Auger recombination is small enough in these samples to be neglected in Eqn. 2.

Plotting $1/\tau_{eff}$ *vs.* 2/w as shown in Fig. 7 shows that s is about 375 cm/s at the $Al_{0.25}Ga_{0.25}In_{0.50}P/Ga_{0.50}In_{0.50}P$ interface in the nid samples, for both ordered and

disordered GaInP. The ordered GaInP DH that was measured to have a τ_{eff} of 47 ns in Fig. 5a is seen to have a bulk lifetime of 82 ns after the surface recombination component has been removed. The disordered GaInP-base samples have a lower, but still fairly long bulk lifetime of 27 ns in this experiment.

The bulk lifetime is dominated by SRH recombination in the nid samples, but radiative recombination is significant in the p-type GaInP samples in Fig. 7. Since radiative recombination is a fundamental mechanism depending only on the doping level, minority-carrier injection level, and the radiative recombination coefficient B, while SRH recombination is mediated by trap levels in the bandgap and hence can be reduced by minimizing defects in the crystal lattice, it is important to separate the effects of radiative and SRH lifetime. The radiative lifetime is calculated from B and the p-type dopant concentration N_A in the GaInP base from:

$$\tau_{\text{bulk,rad}} = \frac{1}{BN_A} \tag{3}$$

resulting in $\tau_{bulk,SRH}$ of 22 ns compared to $\tau_{bulk,total}$ of 14 ns in these p-type samples. The value of s is lower in the p-type samples at ~170 cm/s.

The radiative recombination places an upper limit on the V_{oc} of direct-bandgap solar cells, and this limit was used to calculate the theoretical V_{oc} and efficiency of 3-junction solar cells in Fig. 8, as a function of the bandgap of the GaInAs middle and the GaInP top subcells. The indium compositions of the middle and top subcells were chosen to match a given lattice constant, and the bandgaps were determined from this In composition for GaInAs and disordered GaInP. The radiative limit of the V_{oc} of a single subcell is given by:

$$V_{\text{oc}} = \frac{kT}{q}\ln\left(\frac{J_{\text{ph}}}{qn_i^2 wB}\right) = \frac{kT}{q}\left[\ln\left(\frac{J_{\text{ph}}}{qw}\right) - \ln\left(n_i^2\right) - \ln(B)\right] \tag{4}$$

where J_{ph} is the photogenerated current density, w is the thickness of the solar cell base, n_i is the intrinsic carrier concentration, and the other symbols have their usual meaning. The exponential dependence of n_i on bandgap E_g results in a linear dependence of the $\ln(n_i^2)$ term for V_{oc} on E_g, while the other two log terms in Eqn. 4 are only weakly dependent on E_g. B varies with the square of E_g or more slowly[10]. Even taking into account the dependence of B on E_g, the difference (E_g/q)-V_{oc} between the bandgap voltage and open-circuit voltage varies only from ~0.32 to 0.36 V in the radiative limit, for bandgaps ranging from 1.0 to 1.9 eV, a useful observation when designing multijunction solar cells. The calculated V_{oc} in Fig. 8 thus has a nearly constant offset from the bandgap. J_{ph} increases as the bandgap of the middle cell decreases (see Fig. 1) up to the point at which the middle cell transmission of light begins to starve the Ge bottom cell of current. The increase in current is greater than the effect of decreasing voltage initially, resulting in a maximum theoretical efficiency at a lattice constant corresponding to ~12%-In GaInAs, though most of the available gain can be achieved by 8%-In GaInAs.

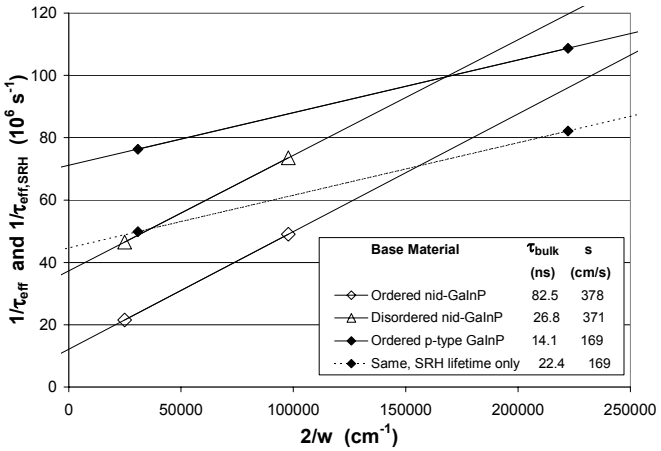

Fig. 7. Extraction of bulk and interface recombination components from TRPL measurements on double heterostructures of various thicknesses.

Experimental V_{oc} and efficiency values are also plotted in Fig. 8, for In compositions ranging from 0 to 15% in the GaInAs middle cell. All data is for fully-processed 3-junction cells with anti-reflection (AR) coating, except the data for 15%-In GaInAs cells (5.715 Å lattice constant), which are based on 2-junction, non-AR-coated GaInP/GaInAs cells. V_{oc} tends to decrease with decreasing bandgap, but has a local maximum at the lattice constant of 1%-In GaInAs, due to the low concentration of defects and correspondingly long lifetime that comes with near perfect lattice match to the Ge substrate, as seen in the TRPL measurements of DHs. The theoretical treatment of V_{oc} in Eqn. 4 and Fig. 8 does not account for the change in crystal defect density with lattice constant, and hence does not show such a maximum. Even the small lattice mismatch of about 0.07% between GaAs and Ge is large enough to have a significant effect on recombination in GaAs grown on Ge. Adding a 1% indium mole fraction to form a $Ga_{0.99}In_{0.01}As$ middle cell increases the V_{oc} of the middle cell significantly by ~70 mV, in spite of the decrease of 15 meV in the bandgap of $Ga_{0.99}In_{0.01}As$ compared to that of GaAs.

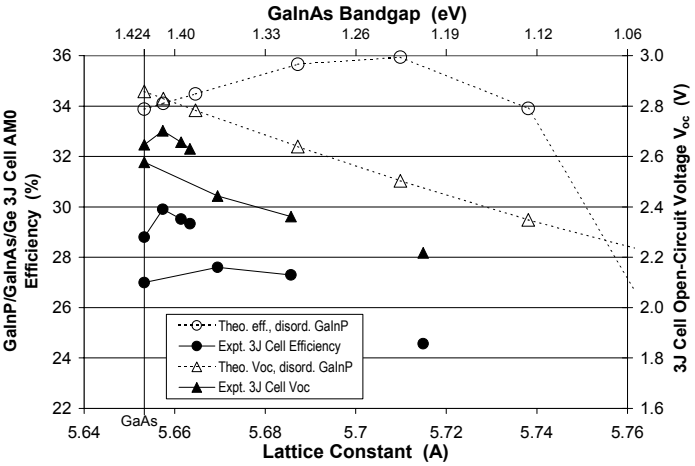

Fig. 8. Theoretical and experimental 3-junction cell efficiency and V_{oc} as a function of lattice constant of the GaInAs middle and GaInP top cells.

Efficiency shows a similar peak at 1%-In GaInAs, and as In content is increased, the efficiency does not fall off as rapidly as V_{oc} due to the greater current available for lower middle cell bandgaps. For example, the slightly lower bandgap of ~1.41 eV for $Ga_{0.99}In_{0.01}As$, compared to 1.424 eV for GaAs, increases the photogenerated current density in the middle cell, taking it from the wasted excess current density of the Ge bottom cell.

Wide-Bandgap Tunnel Junctions

Higher bandgap tunnel junction layers are used to minimize photogeneration in these regions of low minority-carrier collection. However, the higher bandgaps will increase the energy barrier for tunneling, and can have a dramatic effect on tunneling probability and current. Particularly for concentrator cells, with current densities typically hundreds of times that at one sun, the current through the tunnel junction must be kept far below the peak tunneling current to avoid excessive voltage drops across the tunnel junction. The I-V characteristic of a wide-bandgap tunnel junction test structure is plotted in Fig. 9, showing the peak tunneling current and typical one-sun current density. Band offsets at the AlGaAs/GaInP Type-II heterojunction (staggered bandgaps) are such that the slopes of the conduction and valence bands are made steeper, and the space-charge region at the tunnel junction is made narrower thereby increasing the tunneling probability, when the polarity of the tunnel junction is p-AlGaAs/n-GaInP[11].

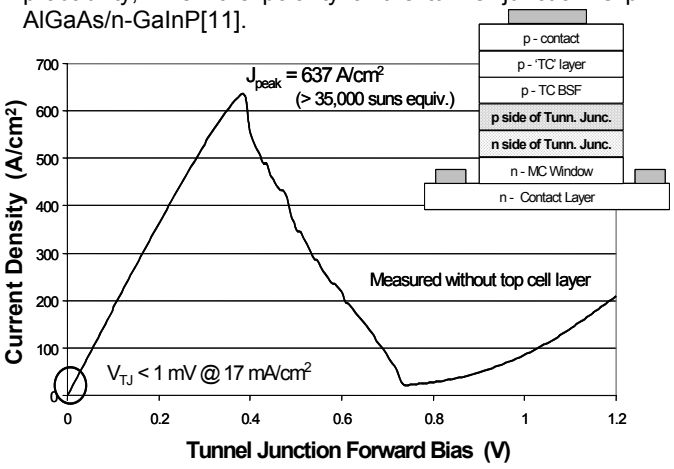

Fig. 9. Current-voltage characteristic of wide-bandgap tunnel junction, showing negligible voltage drop at one sun, and >35,000 suns equivalent peak tunneling current.

High-Efficiency Solar Cells

Implementation of the observations discussed above on bandgap control and crystallinity, in addition to other device improvements, have led to new heights in multijunction cell efficiency. The high conductivity of an optimized wide-bandgap tunnel junction, in addition to its increased transparency, contributes to the record 34% efficiency Spectrolab terrestrial concentrator cell in Fig. 10 (1.0 cm^2, AM1.5G, 15-40 W/cm^2, 25°C). This is the first monolithic solar cell of any type with output power greater than one-third of the power of the sunlight falling on the cell, a necessary step toward meeting the Department of

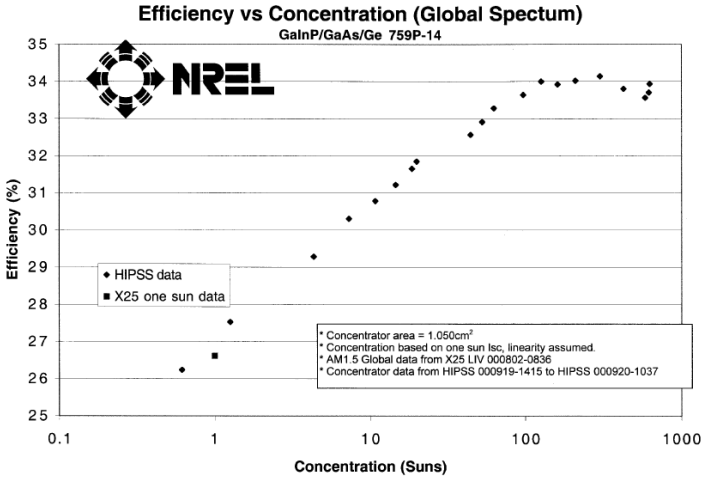

Fig. 10. Performance of a 3-junction Spectrolab terrestrial concentrator cell with 34% efficiency (1.0 cm^2, AM1.5G, 15-40 W/cm^2, 25°C) measured at NREL, as a function of incident intensity.

Energy's "One-Third-of-a-Sun" efficiency milestone at the module level. The high efficiency of this cell testifies to the suitability of wide-bandgap tunnel junctions even at the very high current densities of concentrator cells. Although originally designed for the global spectrum, the AM1.5G spectrum has been found to be a far better spectral match for light imaged onto concentrator cells in most applications[12]. III-V multijunction concentrator cells are proving to be not only very high in efficiency, but also capable of robust operation in practical systems[13-15].

Bandgap control and improved crystallinity, in addition to wide-bandgap tunnel junctions, have allowed a new record efficiency of 29.7% for the space one-sun cell in Fig. 11 (4.0 cm^2, AM0, 0.1353 W/cm^2, 28°C). A light I-V curve for a typical Improved Triple-Junction (ITJ) production solar cell with 26.8% efficiency is shown for comparison[16]. The champion efficiency cell in Fig. 11 is an experimental 4 cm^2 cell from the development of the next-generation production cell at Spectrolab, dubbed the

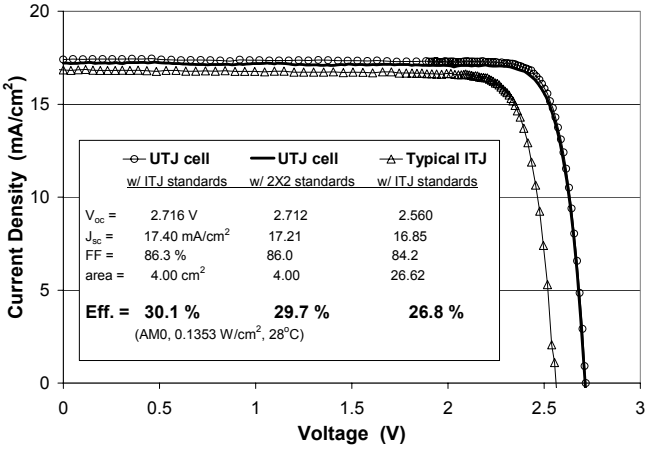

Fig. 11. Light I-V curve of highest AM0 efficiency cell measured at 30.1% (4.0 cm^2, AM0, 0.1353 W/cm^2, 28°C) using the same full-size (26.62 cm^2) balloon-flight standard reference cells used for production ITJ solar cells, and 29.7% using more recent 4-cm^2 balloon-flight standards.

Ultra Triple-Junction (UTJ) cell. When measured with the same large-area (>26 cm^2) current reference cells used to measure the ITJ production cells, the efficiency measured for the same UTJ champion cell is over 30% efficient.

Data from an experimental lot of UTJ cells is shown in Fig. 12, with a very high average AM0 efficiency of 29.0%, average V_{oc} of nearly 2.7 V, and a very tight efficiency distribution. Owing largely to this very high efficiency at beginning of life (BOL), prototype UTJ cells have demonstrated end-of-life (EOL) AM0 efficiencies over 25.5% after irradiation with 1-MeV electrons at a fluence of 5 X 10^{14} e^-/cm^2, and over 24.4% at 1 X 10^{15} e^-/cm^2.

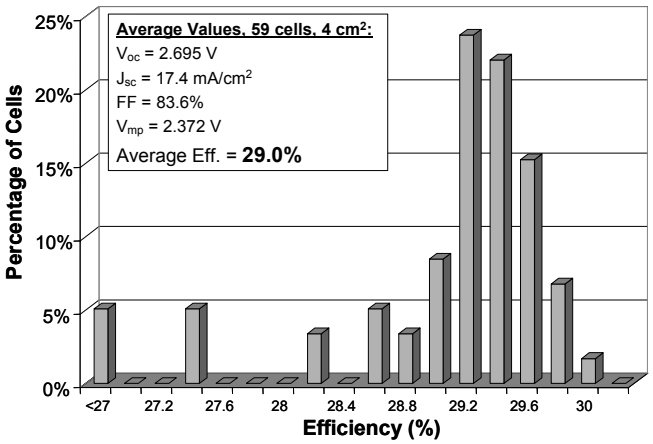

Fig. 12. AM0 efficiency distribution of an experimental lot of 2 cm X 2 cm Ultra Triple-Junction (UTJ) cells.

Conclusions

Increasing the bandgap of the GaInP top cell and tunnel junction layers, while decreasing the bandgap of the GaInAs middle cell and simultaneously reducing dislocation density in the middle cell, has led to new heights in conversion efficiency of 3-junction GaInP/GaInAs/Ge solar cells. For terrestrial concentrators, 3-junction cell efficiencies of 34% have been independently confirmed at the National Renewable Energy Laboratory (NREL) from 150 to 400 suns. For space applications, these device improvements have resulted in efficiencies approaching 30% for the AM0 spectrum. These increases in efficiency translate directly into improved cost-effectiveness for both space and earth-based solar power.

Acknowledgments

The authors would like to thank Clay Mayberry, Kitt Reinhardt (now at NASA) and Donna Senft of the Air Force Research Laboratory, Dean Marvin of the Aerospace Corporation, Keith Emery and Tom Moriarty for cell efficiency measurements at NREL, Brian Keyes at NREL for TRPL measurements, Dick Ahrenkiel, Dan Friedman, and Sarah Kurtz of NREL for helpful discussions, and Mark Takahashi, Raed Sherif, and the entire multijunction solar cell team at Spectrolab. This work was supported in part by the Air Force Research Laboratory (AFRL/VS) under DUS&T contract # F29601-98-2-0207, and by Spectrolab.

References

[1] J. M. Olson, S. R. Kurtz, A. E. Kibbler, and P. Faine, "A 27.3% Efficient $Ga_{0.5}In_{0.5}P$/GaAs Tandem Solar Cell," *Appl. Phys. Lett.*, **56**, p. 623 (1990).

[2] R. R. King, N. H. Karam, J. H. Ermer, M. Haddad, P. C. Colter, T. Isshiki, H. Yoon, H. L. Cotal, D. E. Joslin, D. D. Krut, R. Sudharsanan, K. M. Edmondson, B. T. Cavicchi, and D. R. Lillington, "Next-Generation, High-Efficiency III-V Multijunction Solar Cells," *Proc. 28th IEEE Photovoltaic Specialists Conf.* (IEEE, New York, 2000), p. 998.

[3] R. R. King, M. Haddad, T. Isshiki, P. C. Colter, J. H. Ermer, H. Yoon, D. E. Joslin, and N. H. Karam, "Metamorphic GaInP/GaInAs/Ge Solar Cells," *Proc. 28th IEEE Photovoltaic Specialists Conf.* (IEEE, New York, 2000), p. 982.

[4] F. Dimroth, U. Schubert, and A. W. Bett, "25.5% Efficient Ga0.35In0.65P/Ga0.83In0.17As Tandem Solar Cells Grown on GaAs Substrates," *IEEE Electron Device Lett.*, **21**, p. 209 (2000).

[5] D. J. Friedman, J. F. Geisz, Sarah R. Kurtz, and J. M. Olson, "1-eV GaInNAs Solar Cells for Ultrahigh-Efficiency Multijunction Devices," *Proc. 2nd World Conf. on Photovoltaic Solar Energy Conversion* (European Commission, Ispra, Italy), p. 3.

[6] S.R. Kurtz, A.A. Allerman, E.D. Jones, J.M. Gee, J.J. Banas, and B.E. Hammons, "InGaAsN Solar Cells with 1.0 eV Band Gap, Lattice Matched to GaAs," *Appl. Phys. Lett.*, **74**, p. 729 (1999).

[7] D. J. Friedman, J. F. Geisz, K. A. Emery, Sarah R. Kurtz, "Critical Analysis of the GaInP/GaAs/1-eV/Ge Cell for Terrestrial Concentrator Application," *to be publ. in Proc. 29th IEEE Photovoltaic Specialists Conf.* (IEEE, New York, 2002).

[8] Sarah R. Kurtz, R. R. King, K. M. Edmondson, D. J. Friedman, and N. H. Karam, "1-MeV-Electron Irradiation of GaInAsN Cells," *to be publ. in Proc. 29th IEEE Photovoltaic Specialists Conf.* (IEEE, New York, 2002).

[9] M. W. Wanlass, T. J. Coutts, J. S. Ward, K. A. Emery, T. A. Gessert, and C. A. Osterwald, "Advanced High-Efficiency Concentrator Tandem Solar Cells," *Proc. 22nd IEEE Photovoltaic Specialists Conf.* (IEEE, New York, 1991), p. 38.

[10] R. K. Ahrenkiel in *Minority Carriers in III-V Semiconductors: Physics and Applications, Semiconductors and Semimetals*, **39**, (Academic Press, New York, 1993), R.K. Ahrenkiel and M. S. Lundstrom, eds., Chap. 2, pp. 39-149.

[11] D. Jung, C. A. Parker, J. Ramdani, and S. M. Bedair, "AlGaAs/GaInP Heterojunction Tunnel Diode for Cascade Solar Cell Application," *J. Appl. Phys.*, **74**, p. 2090 (1993).

[12] K. Emery, "What is the Appropriate Reference Condition for Determining the Efficiency?," *NCPV Program Review Meeting* (AIP Press, Woodbury, NY, 2001).

[13] H. Cotal, R. Sherif, G. Glenn, D. Krut, A. Paredes, T. Meza, and H. Hayden, "High Concentration Testing and Performance of Multijunction Solar Cells," *to be publ. in Proc. 29th IEEE Photovoltaic Specialists Conf.* (IEEE, New York, 2002).

[14] R. Sherif et al., "A 2-kW Concentrating PV Array Using Triple-Junction Cells," *to be publ. in Proc. 29th IEEE Photovoltaic Specialists Conf.* (IEEE, New York, 2002).

[15] A. P. Stavrides, R. R. King, P. C. Colter, G. Kinsey, A. J. McDanal, M. J. O'Neill, and N. H. Karam, "Fabrication of High-Efficiency, III-V Multijunction Solar Cells for Space Concentrators," *to be publ. in Proc. 29th IEEE Photovoltaic Specialists Conf.* (IEEE, New York, 2002).

[16] J. E. Granata, J. H. Ermer, P. Hebert, M. Haddad, R. R. King, D. D. Krut, M. S. Gillanders, N. H. Karam, and B. T. Cavicchi, "Advancements in $GaInP_2$/GaAs/Ge Solar Cells – Production Status, Qualification Results and Operational Benefits," *to be publ. in Proc. 29th IEEE Photovoltaic Specialists Conf.* (IEEE, New York, 2002).